Journal of Thermal Analysis, Vol. 35 (1989) 2297–2303

ON THE THERMAL DECOMPOSITION OF $Zn(NO_3)_2 \cdot 6H_2O$ AND ITS DEUTERATED ANALOGUE

M. Maneva and *N. Petrov*

DEPARTMENT OF INORGANIC CHEMISTRY, HIGHER INSTITUTE OF CHEMICAL TECHNOLOGY, 8 KLIMENT OHRIDSKI STREET, 1156 SOFIA, BULGARIA

(Received August 30, 1988; in revised form July 8, 1989)

The thermal dehydration and decomposition of $Zn(NO_3)_2 \cdot 6H_2O$ (I) were studied via DTA, TG and DSC, quantitative analysis and IR spectroscopy, and compared with those of $Zn(NO_3)_2 \cdot 6D_2O$ (II). The following phase transitions were observed: melting of the salts; partial dehydration to tetrahydrate; formation of basic nitrate-hydrate; and formation of ZnO.

The sum of the enthalpies of dehydration and thermal decomposition for I was 286 kJ/mol, while that for II was 299 kJ/mol (data from DSC). The probable mechanisms were determined from the TG curves and the formal kinetic parameters were calculated for the two stages of thermal decomposition. Calculations with an equation of the accelerating-type exponential law gave for the formation of basic zinc nitrate-hydrate $E^* = 59$ kJ/mol for I and $E^* = 64$ kJ/mol for II. For the decomposition of the basic salt, the equation for bidimentional diffusion yielded $E^* = 127$ kJ/mol for I and $E^* = 138$ kJ/mol for II.

The literature includes [1–4] on investigation of the thermal decomposition of $Zn(NO_3)_2 \cdot 6H_2O$ via DTA and TG. Three endoeffects have been observed: the first relates to the melting of the salt in its crystallization water. The conclusions on the second differ: according to [1] it is due to complete dehydration to anhydrous $Zn(NO_3)_2$, while [2, 3] consider that it relates to partial dehydration and thermal decomposition to basic zinc nitrate. The partial dehydration proceeds to a trihydrate in [2], and to a dihydrate in [3]. The third endoeffect corresponds to the decomposition of the intermediate to ZnO.

The purpose of the present investigation was to survey the processes of thermal dehydration and decomposition of $Zn(NO_3)_2 \cdot 6H_2O$, to compare them with those of $Zn(NO_3)_2 \cdot 6D_2O$, to determine the enthalpies of the phase transitions by means of DSC and to calculate the kinetic parameters of the process from the data of the TG curves.

John Wiley & Sons, Limited, Chichester
Akadémiai Kiadó, Budapest

Experimental

The initial $Zn(NO_3)_2 \cdot 6H_2O$ (I) was obtained by double recrystallization of $Zn(NO_3)_2 \cdot 6H_2O$, p.a. grade, while $Zn(NO_3)_2 \cdot 6D_2O$ (II), was obtained by multiple recrystallization from heavy water.

The DTA and TG curves were recorded on a Netzsch–429 apparatus at heating rates of 2 deg/min and 5 deg/min in open ceramic crucibles from 20° to 400°. Under the same conditions, with a heating rate of 5 deg/min, intermediates were isolated at 40°, 160°, 210°, 240° and 285° for I, and at 40°, 155°, 215°, 240° and 280° for II. The initial samples weighed 100 mg.

The initial compound and the intermediates were identified by quantitative analysis: zinc complexometrically [5], nitrate spectrophotometrically on a Perkin–Elmer 323 instrument, and water by Fischer's method [6].

The IR spectra of all samples were taken on an R–10 spectrophotometer, in a suspension of nujol in the range 3800–400 cm^{-1}, and in Hostaflen in the range of 3800–1400 cm^{-1}. The intermediates were resinous and highly hygroscopic, which is why the damples were prepared in the above solvents.

Results and discussions

The DTA and TG data relating to heating rates of 2 and 5 deg/min are presented in Figs 1 and 2, respectively. Table 1 shows the temperatures for the most important phase transitions, the corresponding weight changes, and the probable chemical pattern of the process.

The quantitative analysis data on the intermediates are presented in Table 2, and the DSC data in Table 3.

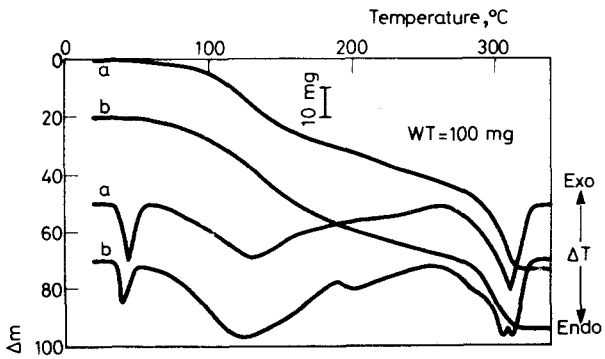

Fig. 1 DTA and TG curves at a heating rate of 2 deg/min: curves *a* for $Zn(NO_3)_2 \cdot 6H_2O$, curves *b* for $Zn(NO_3)_2 \cdot 6D_2O$

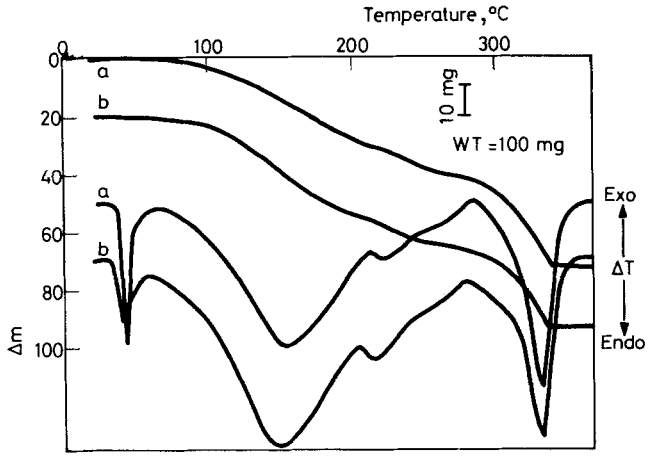

Fig. 2 DTA and TG curves at a heating rate of 5 deg/min: curves *a* for $Zn(NO_3)_2 \cdot 6H_2O$, curves *b* for $Zn(NO_3)_2 \cdot 6D_2O$

Table 1 DTA and TG data for I and II at different heating rates

Phase transition	Form	2 deg/min				5 deg/min			
		Δm, %	T_{init}, °C	T_{fin}, DTA	T_{max}, °C	Δm, %	T_{init}, °C	T_{fin}, DTA	T_{max}, °C
$Zn(NO_3)_2 \cdot 6H_2O(s) \rightarrow$	H	0	30	55	44	0	30	68	42
$\rightarrow Zn(NO_3)_2 \cdot 6H_2O(l)$	D	0	30	50	40	0	30	55	40
$Zn(NO_3)_2 \cdot 6H_2O(l) \rightarrow$	H	42.7	55	265	130	42.6	68	285	155
									225
$\rightarrow xZn(NO_3)_2 \cdot yZn(OH)_2 \cdot zH_2O$	D	46.8	50	258	126				
					198				
$xZn(NO_3)_2 \cdot yZn(OH)_2 \cdot zH_2O \rightarrow$	H	29.9	265	325	312	30.0	285	360	335
$\rightarrow ZnO$	D	26.9	258	325	306	26.9	280	355	332
					316				

The IR spectra are shown in Fig. 3.

The endoeffect observed at 40–44° in the DTA curves of I and II at both heating rates (Figs 1 and 2) corresponds to the melting of the compound in its crystallization water. However, II melts at a lower temperature than I.

The second large endoeffect is related to the weight loss of the sample which, according to [2, 3] is due to dehydration and concomitant hydrolysis to basic zinc nitrate of variable composition. Additional information about the natures of these processes is obtained from the quantitative analysis data and the IR spectra of the

Table 2 Chemical compositions of the initial and intermediate samples during the dehydration and thermal decomposition of I and II at a heating rate of 5 deg/min

Form	T, °C	Δm, %	Chemical composition			Mole ratio
			Zn	NO_3	H_2O	$Zn:NO_3:H_2O$
	40	0	22.0	41.7	36.3	1.0:2.0:6.0
	160	18.2	26.9	50.9	22.2	1.0:2.0:3.0
H	210	29.5	30.8	51.6	15.5	1.0:1.8:1.8
	240	35.5	34.1	54.7	8.4	1.0:1.7:0.9
	285	42.7	38.4	53.0	3.1	1.0:1.5:0.3
	40	0	21.1	40.1	38.8	1.0:2.0:6.0
	155	19.4	26.2	49.7	24.1	1.0:2.0:3.0
D	215	35.3	32.6	55.4	10.1	1.0:1.9:1.0
	240	42.3	36.7	57.1	3.2	1.0:1.6:0.3
	280	46.8	39.6	52.0	1.7	1.0:1.4:0.1

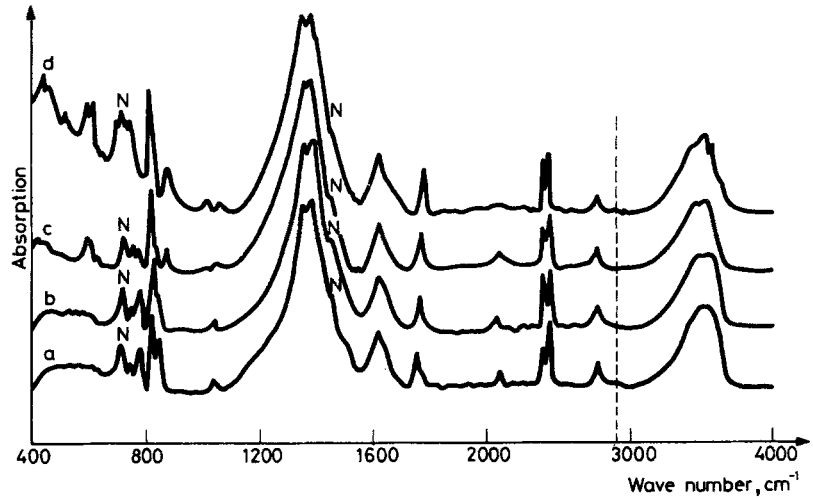

Fig. 3 IR spectra of $Zn(NO_3)_2 \cdot 6H_2O$: *a* – the initial material and the intermediates; *b* – at 210°; *c* – at 240°; *d* – at 285°

intermediates obtained in the given temperature range. The samples taken at 160° for I and 155° for II show that at these temperatures (corresponding to the maximum of the effect described) the compositions correspond to $Zn(NO_3)_2 \cdot 3H_2O$ and $Zn(NO_3)_2$–$3H_2O$, respectively (Table 2, Fig. 3, curves *a* and *b*), i.e. at the beginning partial dehydration occurs in the melt. The preparation of these intermediate hydrates is not registered by a separate effect in the DTA curve, nor by a visible change in the TG curve. This shows that the end of the dehydration

process is linked to the beginning of hydrolysis. Such an assumption is confirmed by the data about the subsequent intermediates, i.e. those at 210° for I and 215° for II. A disturbance of the mole ratio $Zn:NO_3$ is observed (Table 2), while in the IR spectrum of I (Fig. 3, curve *c*) there is a slight absorption band at 886 cm^{-1}. This is to be expected, since the quantity of the hydrolysate is still negligible. Confirmation is provided by the weak effect in the DTA curve in this range (Fig. 2). It can be explained by the fact that, simultaneously with the hydrolysis, sufficient dehydration occurs in the system to compensate for the exoeffect due to hydrolysis.

The data in the subsequent intermediates at 240° for I and II (Table 2) show the further course of the hydrolysis and a decrease in the water in the system. The IR spectrum of this sample for I (Fig. 3) shows the characteristic absorption bands of the Zn–OH group. The weak absorption at 1070 and 1060 cm^{-1} can be attributed to the in-plane deformation vibration Zn–OH. Such an intensity is to be expected, considering the ionic-covalent character of the Zn–OH bond determining the absorption at 620 cm^{-1}. The absorption at 886 cm^{-1} in the spectrum of that sample (Fig. 3, *c*), which further increases in intensity (Fig. 3, *d*), can be attributed to the out-of-plane deformation vibration of the group examined. The presence of water molecules in the composition of the intermediate and the participation in strong hydrogen-bonds is proved by the vibrational variations observed at 795 and 775 cm^{-1}. The position of the latter is calculated from the composite vibration at 2420 and 2400 cm^{-1}, which is the sum of $\delta_{H_2O}+\nu_L$.

The next sample, at 285° for I and at 280° for II, completes the endoeffect examined. The compositions of the samples then correspond to mole ratios of $Zn: NO_3:H_2O = 1.0:1.5:0.3$ for I and $1.0:1.4:0.1$ for II.

The IR spectrum of the sample at 240° for I (Fig. 3, curve *d*) is analogous to that of the sample at 210° (Fig. 3, curve *c*).

The endoeffect with maximum at 355° for I and at 332° for Ii corresponds to the decomposition of the basic zinc nitrate to zinc oxide.

It is noteworthy that the beginning of the third endoeffect and its maximum for II (Fig. 2) are observed at lower temperatures than those for I. This dependence is seen in Fig. 1 (at a heating rate of 2 deg/min), though at considerably lower temperatures.

When the data from Fig. 1 are compared with those from Fig. 2, it becomes obvious that the heating rate affects essentially the temperatures of the phase transitions.

The DSC curves for I and II display three endoeffects analogous to those from DTA. The enthalpies of these phase transitions are presented in Table 3. They differ considerably from those calculated on the basis of Hess's thermochemical law, e.g. for the second endoeffect for I, ΔH° = 189 kJ/mol, while the calculated value is 355 kJ/mol; for II, the corresponding data are 196 kJ/mol and 360 kJ/mol,

respectively. A comparison of the ratios of the determined and calculated enthalpies of the second endoeffect for I and II demonstrates that for both compounds under the DSC conditions hydrolysis takes place to the same degree (196/189 : 360/355 = 1.04 : 1.01). The small difference in the determined enthalpies for I and II (Table 3) in the two phase transitions is due to differences in the evaporation enthalpies of H_2O and D_2O.

On the basis of the TG data (Fig. 1), the probable mechanisms were proposed and the kinetic parameters (E and Z) were determined separately for the dehydration process and the concomitant hydrolysis to basic nitrate-hydrate (stage A) and its decomposition to zinc oxide (stage B). They were calculated by means of a computer program based on an algorithm discussed in [7]. The data for stage A are described by the kinetic equation

$$F(\alpha) = \alpha$$

The data for stage B are described by the kinetic equation:

$$F(\alpha) = [-\ln(1-\alpha)]^{-1}$$

Calculated for stage A:

$E^* = 59$ kJ/mol $\quad Z = 5.2 \times 10^8\ s^{-1}$ for I;

$E^* = 64$ kJ/mol $\quad Z = 3.7 \times 10^8\ s^{-1}$ for II.

Calculated for stage B:

$E^* = 127$ kJ/mol $\quad Z = 1.1 \times 10^{10}\ s^{-1}$ for I;

$E^* = 138$ kJ/mol $\quad Z = 6.2 \times 10^{10}\ s^{-1}$ for II.

References

1 G. G. Urazov, A. K. Kirakosjan and R. S. Mhitarjan, Zh. Neorg. Khim., 2 (1958) 491.

2 A. M. Sirina, I. I. Kalinichenko and A. I. Purtov, Zh. Neorg. Khim., 9 (1970) 2430.

3 T. Djuraeva, V. K. Hakimova and M. T. Saibova, Uzb. Khim. Zh., 2 (1972) 3.

4 D. Weigel, B. Imelik and M. Prettre, C. R. Hebd. Seancas Acad. Sci., 259 (1964) 2215.

5 Komplexometrische Bestimmungsmethoden mit Titriplex, E. Merck AG, Darmstadt.

6 Bulg. State Standard 6730–74.

7 A. Bhatti and D. Dollimore, Thermochim. Acta, 78 (1984) 55–62.

Zusammenfassung — Mittels DTA, TG, DSC, Elementaranalyse und IR-Spektroskopie wurde die thermische Dehydratation und Zersetzung von $Zn(NO_3)_2 \cdot 6H_2O$ (I) untersucht und mit der von $Zn(NO_3)_2 \cdot 6D_2O$ (II) verglichen. Folgende Phasenumwandlungen konnten beobachtet werden: Schmelzen des Salzes; teilweise Dehydratation zu Tetrahydrat; Bildung von basischem Nitrathydrat; und Bildung von ZnO. Die Summe der Enthalpien für Dehydratation und Zersetzung betrug für I 286 kJ/mol und für II 299 kJ/mol (berechnet aus DSC). Die wahrscheinlichen Mechanismen wurden auf Grundlage der TG-Kurven festgelegt und die formalen kinetischen Parameter für die zwei Schritte der thermischen Zersetzung berechnet. Berechnungen ergaben für die Bildung des basischen Zinknitrathydrates $E_m^* = 59$ kJ/mol bei I und $E^* = 64$ kJ/mol für II. Für die Zersetzung des basischen Salzes lieferte eine Gleichung für zweidimensionale Diffusion $E^* = 127$ kJ/mol für I und $E^* = 138$ kJ/mol für II.

Резюме — Методами ДТА, ТГ, ДСК, ИК спектроскопии и качественного анализа изучены термическая дегидратация и разложение гексагидрата нитрата цинка (I). Полученные данные сопоставлены с таковыми для его дейтеропроизводного (II). Наблюдались следующие фазовые превращения; плавление обеих солей, частичная дегидратация до тетрагидрата, образование основной нитрат-гидратной соли и конечное образование оксида цинка. Исходя из данных ДСК, сумма энтальпий процесса дегидратации и термического разложения для I составляла 286 кдж·моль$^{-1}$, а для II 299 кдж·моль$^{-1}$. На основе ТГ кривых определены возможные механизмы разложения, а для двух стадий термического разложения были вычислены также формальные кинетические параметры. Вычисления, проведенные с помощью уравнения ускоряющего экспоненциального закона, дали значения E^* образования основной соли цинка для I – 59 кдж·моль$^{-1}$, а для II – 64 кдж·моль$^{-1}$. Значения E^* процесса разложения основной соли, найденные с помощью уравнения двуразмерной диффузии, составляли для I и II, соответственно, 127 и 138 кдж·моль$^{-1}$.